AMERICAN SOCIETY FOR MICROBIOLOGY | Infection and Immunity®

HOST RESPONSE AND INFLAMMATION

The Reaction of Innate Lymphoid Cells in the Mouse Female Genital Tract to Chlamydial Infection

Svenja Barth,[a] Susanne Kirschnek,[a] Noemi Ortmann,[a] Yakup Tanriver,[a] Georg Häcker[a,b]

[a]Faculty of Medicine, Institute of Medical Microbiology and Hygiene, Medical Center, University of Freiburg, Freiburg, Germany
[b]BIOSS Centre for Biological Signalling Studies, University of Freiburg, Freiburg, Germany

ABSTRACT Innate lymphoid cells (ILCs) comprise five distinct subsets. ILCs are found at mucosal barriers and may fight invading pathogens. *Chlamydia* is an intracellular bacterium that infects the mucosa of the genital tract and can cause severe tissue damage. Here, we used a mouse infection model with *Chlamydia muridarum* to measure the reaction of genital tract ILCs to the infection. Tissue-resident natural killer (NK) cells were the largest group in the uninfected female genital tract, and their number did not substantially change. Conventional NK cells were present in the greatest numbers during acute infection, while ILC1s continuously increased to high numbers. ILC2 and ILC3s were found at lower numbers that oscillated by a factor of 2 to 4. The majority of ILC3s transdifferentiated into ILC1s. NK cells and ILC1s produced gamma interferon (IFN-γ) and, rarely, tumor necrosis factor (TNF), but only early in the infection. Lack of B and T cells increased ILC numbers, while the loss of myeloid cells decreased them. ILCs accumulated to a high density in the oviduct, a main site of tissue destruction. ILC subsets are part of the inflammatory and immune reaction during infection with *C. muridarum* and may contribute to tissue damage during chlamydial infection.

KEYWORDS *Chlamydia*, genital infection, innate lymphoid cells, tissue damage

Chlamydia trachomatis is the most common agent of sexually transmitted bacterial disease worldwide. The prevalence of *C. trachomatis* in young adults is in the order of 3% to 5%, and the global yearly incidence is about 130 million cases (1, 2). The main clinical problem of genital infection with *C. trachomatis* is the propensity of the bacteria to ascend through the female genital tract, with the potential of permanent tissue damage and infertility and ectopic pregnancy (3, 4). The inflammatory response is a major contributor to tissue damage (4). The immune reaction is complex, and although it is not well understood in humans (5), animal models agree that *Chlamydia* can be cleared by the immune response (6–8). A number of factors have been identified that contribute to tissue damage as well as to immunity, mostly in the infection model of mice with *Chlamydia muridarum* (9). Depletion of neutrophils reduces tissue damage (10). CD4 as well as CD8 T cells have been implicated in tissue damage (11, 12), and tumor necrosis factor (TNF) signaling appears to play a role (12, 13). A protective role of CD4 T cells during chlamydial infection has also been reported, and the cytokines gamma interferon (IFN-γ) and interleukin 12 (IL-12) contribute to protection (8).

Innate lymphoid cells (ILCs) are lymphocytes lacking diversified T or B cell receptors. ILCs are part of the innate immune system and are currently divided into five cell types. Apart from the lymphoid tissue inducer (LTi) cells, ILCs have equivalents in the T-cell lineage, with one cytotoxic cell type (natural killer [NK] cells) and three cell types with particular specificities in terms of cytokine production (ILC1 to ILC3, producing a similar pattern of cytokines as TH1, TH2, and TH17 cells) (14). ILCs, with the exception of NK cells, are scarce in lymphoid organs but are mostly present at mucosal surfaces (14).

Citation Barth S, Kirschnek S, Ortmann N, Tanriver Y, Häcker G. 2021. The reaction of innate lymphoid cells in the mouse female genital tract to chlamydial infection. Infect Immun 89:e00800-20. https://doi.org/10.1128/IAI.00800-20.

Editor Craig R. Roy, Yale University School of Medicine

Address correspondence to Georg Häcker, georg.haecker@uniklinik-freiburg.de.

Received 21 December 2020
Returned for modification 12 March 2021
Accepted 9 August 2021
Accepted manuscript posted online 23 August 2021
Published 15 October 2021

The reason for this localization is not entirely clear (15), but one interpretation is that ILCs have a role in defense against pathogens invading through these surfaces; a number of examples for this activity have been reported in experimental infections of the lung or the intestine (16). All types of ILCs are present in differing numbers in the mouse female genital tract (17). The two known types of NK cells, conventional NK (cNK) and tissue-resident NK (trNK) cells show substantial variation in the uterus depending on sexual maturity (18), and mice lacking NK cells had a higher viral load upon genital infection with herpes simplex virus (19). A direct antibacterial activity of NK cells *in decidua* has recently been described (20). Depletion of NK cells was associated with a loss of early IFN-γ production during infection and an exacerbation of the *C. muridarum* infection (21), although this study has the limitation that the depletion method used (anti-asialo-GM1 antibodies) also affects other cell populations, such as ILC1s, some T cells, and basophils. A recent study investigated the role of ILCs by comparing RAG-deficient mice (which have no T or B cells) with RAG/IL-2R common γ-chain-deficient mice (which additionally have no ILC) and found a role of ILCs as producers of IFN-γ in containing the human pathogen *Chlamydia trachomatis* (22) during mouse infection. Indeed, the transfer of ILC3-like cells could protect mice from intestinal colonization with a *C. muridarum* mutant strain that was sensitive to IFN-γ (23). We provide here a detailed study of the dynamics and activity of the various ILC populations in the murine female genital tract (FGT) in response to infection with *C. muridarum*. We found distinct reactions of the various cell populations, which differed between the FGT organs and depended substantially on the presence of myeloid cells.

RESULTS

We measured the numerical dynamics of ILCs in the FGT during *C. muridarum* infection. Bacterial replication starts at the *cervix uteri* and ascends to the upper parts of the FGT, and bacteria are cleared after 3 to 4 weeks (24). We devised a gating strategy to detect ILCs in single-cell suspensions prepared from the whole FGT of mice and were able to identify cNK/trNK cells, ILC1s, ILC2s, and ILC3s by multicolor staining and flow cytometry (see Fig. S1 in the supplemental material). All populations were detectable in uninfected mice (Fig. 1), with NK cells (cNK and trNK; the two groups are discussed separately further below) at about 30,000 cells being by far the largest population. The lowest numbers were found for ILC3s (around 100 cells per FGT). Upon infection, NK cell numbers expanded 2- to 3-fold over the first 3 days and then stayed relatively constant until day 30. When mice were reinfected on day 50, no substantial change in numbers was seen (Fig. 1A). A high interindividual variability was observed at some time points. It is a characteristic of this model that many but not all mice develop a severe inflammatory phenotype, associated with higher numbers of inflammatory cells, and this very likely contributes to the observed variation (see also Fig. 6). ILC1s expanded by a factor of 5 to 10 over 30 days, contracted significantly by day 50, and showed no significant changes upon reinfection (Fig. 1B). There were small changes in the numbers of the ILC2 population; a nonsignificant reduction in cell numbers occurred between days 4 and 7, but the numbers throughout remained around 1,000 to 3,000 cells per total FGT (Fig. 1C). Similarly, ILC3s showed some variation and, overall, even lower numbers, in the range of approximately 100 to 400 cells per FGT (Fig. 1D).

The (small) loss of ILC2s between days 4 and 7 may have been due to apoptosis, and we therefore tested *vav-bcl-2* transgenic mice. These mice express high levels of human Bcl-2 under the *vav* promoter, and all hematopoietic cells investigated have been found to have high Bcl-2 levels (25). We tested the expression of human Bcl-2 in ILCs and found high levels in these cell populations as well, indicating expression of the transgene (Fig. S2A). Most forms of "contractions," i.e., reductions in population size in immune cell populations, are inhibited by Bcl-2 (see for instance reference 26). We found no difference between the strains, suggesting that Bcl-2-inhibitable apoptosis is not involved in the reduction; similarly, day 30 counts of NK cells were not elevated in *vav-bcl-2* mice, arguing against a major role of mitochondrial apoptosis in the turnover of these cells (Fig. S2B to

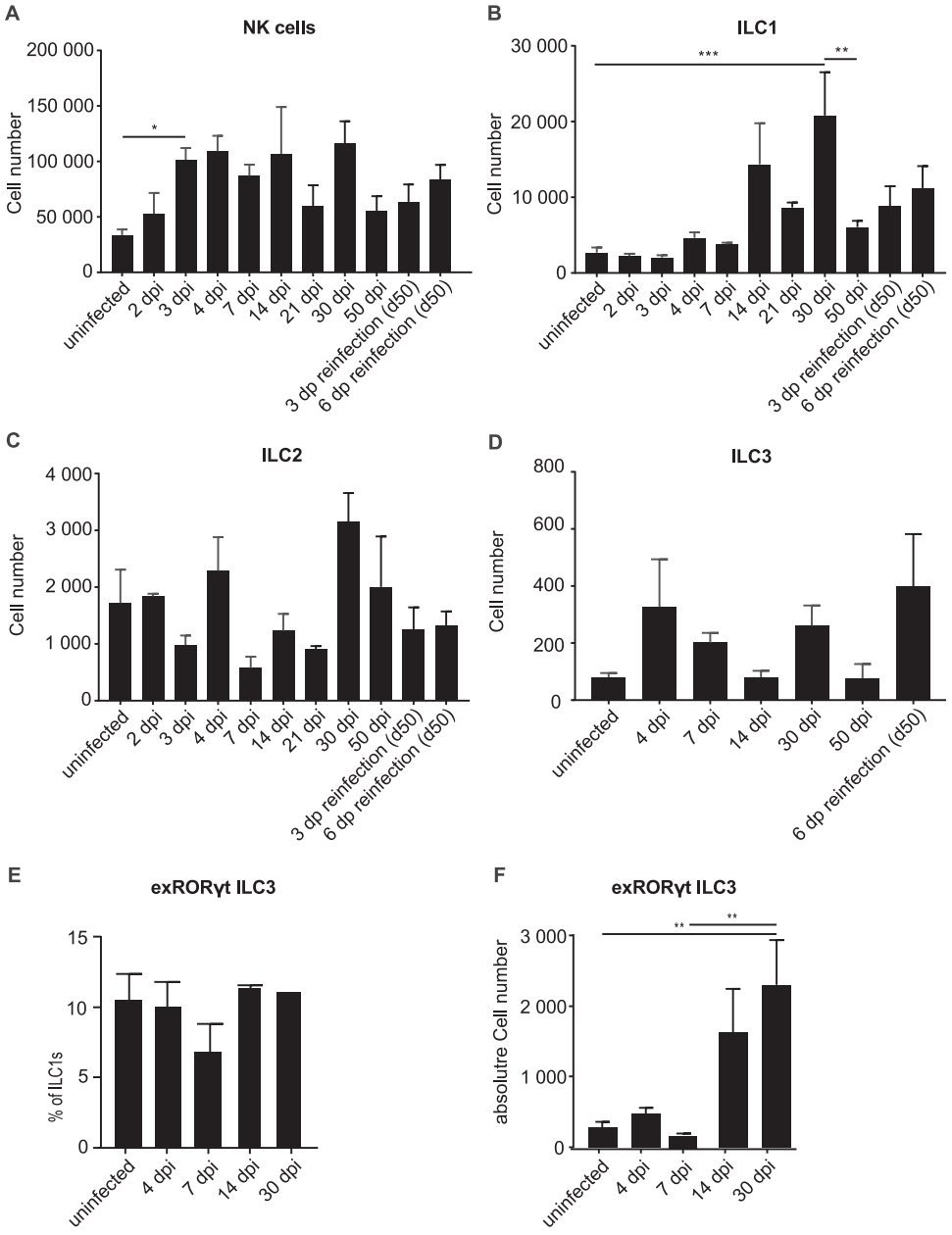

FIG 1 Dynamics of innate lymphoid cell (ILC) numbers in whole FGTs upon infection with *Chlamydia muridarum*. Wild-type (wt) mice were infected intravaginally with 5×10^5 inclusion-forming units (IFUs) of *C. muridarum*. FGTs were isolated at the indicated time points, and leucocytes of whole FGTs were analyzed by immunostaining and subsequent flow cytometry. Absolute cell numbers were obtained by including a defined number of reference beads. (A) Natural killer (NK) cells were defined as $CD45^+$, Lin(CD3, CD5, CD19, TCRβ, TCR$\gamma\delta$, F4/80, FcεR1α, Ly6G)$^-$, $NK1.1^+$, $Eomes^+$ cells. (B) ILC1s were defined as $CD45^+$, Lin^-, $NK1.1^+$, $Eomes^-$ cells. (C) ILC2s were defined as $CD45^+$, Lin^-, $CD127^+$, $ST2^+$, $GATA3^+$ cells. (D) ILC3s were defined as $CD45^+$, Lin^-, $CD127^+$, RORγt^+ cells. Data show mean and standard error of the mean (SEM) of 3 to 9 mice; the numbers of mice and experiments are separately listed in Table S1 in the supplemental material. Significance between means was tested by Tukey's multiple-comparison test (*, $P < 0.05$; other differences were not significant). ILC, innate lymphoid cell; NK, natural killer; dpi, days postinfection. (E, F) *Eomes*$^{GFP/+}$ *Rosa26*$^{YFP/+}$ *Rorc(γt)*-Cre^{tg} mice were infected intravaginally with 5×10^5 IFUs of *C. muridarum*. FGTs were isolated at the indicated time points, and leucocytes of whole FGTs were analyzed via immunostaining and subsequent flow cytometry. Percentage of exRORγt-ILC3s (defined as $CD45^+$, Lin^-, $NK1.1^+$, $Eomes^-$, RORγt-fm$^+$) relative to ILC1s (defined as $CD45^+$, Lin^- $NK1.1^+$, $Eomes^-$) (B) and absolute exRORγt-ILC3 numbers (C) were calculated using absolute ILC1 numbers (Fig. 1B). Data show means and SEM of 2to 6 mice. Significance between means was tested by Sidak's multiple-comparison test (*, $P = 0.05$).

D). There were no significant changes in ILC3 numbers during the observation period. We had expected that ILC3s, which play a role in the defense against a bacterial pathogen in the mouse intestine (27), might also contribute to the reaction during chlamydial infection. ILC3s further can contribute to hyperinflammation in the intestine (28), and an inflammatory effect plays a role in *C. muridarum*-induced tissue damage. ILC3s have the potential to transdifferentiate into ILC1s under the influence of proinflammatory cytokines (29). We therefore considered the possibility that such transdifferentiation was the reason for the lack of ILC3 expansion and used fate map reporter mice to detect such a potential conversion. $Eomes^{GFP/+}$ $Rosa26^{YFP}$ $Rorc^{Cre\text{-}Tg}$ mice permit the identification of all cells that at one stage have expressed the transcription factor RORγt (30). Because RORγt is expressed by ILC3s but lost again if they convert to ILC1s, these mice permit the identification of exRORγt-ILC3s. We infected these mice with *C. muridarum* and measured the number of cells that were phenotypically ILC1 but expressed yellow fluorescent protein (YFP) as a marker of the history of RORγt expression (exRORγt-ILC3s) (31). The relative number of exRORγt-ILC3s as a percentage of all ILC1s was remarkably constant at about 10% throughout the infection (Fig. 1E). Because of the large increase in ILC1s, there was, however, a substantial increase in total cell number to about 2,000 exRORγt-ILC3s on day 30, with exRORγt-ILC3s outnumbering ILC3s by a factor of about five (Fig. 1F). Although relatively few ILC1s had a history as ILC3s, this conversion substantially reduced the numbers of ILC3s and may have been functionally relevant during the course of the infection.

We proceeded to an analysis with higher spatial resolution and analyzed parts of the FGT separately. The infection starts at the cervix and ascends into the uterine horns and eventually into the upper parts of the FGT, comprising oviducts and ovaries (here referred to as oviducts). We divided the FGT and analyzed these parts separately. Depending on the readout, the FGT was analyzed in 3 to 6 parts, as illustrated in Fig. S3. A high load of *C. muridarum* was found in the cervix on days 3 to 7; the number of detectable bacteria declined until day 21, and bacteria were undetectable by day 30 (genome equivalents were quantified by PCR; see Fig. S4). The bacteria spread surprisingly quickly through the uterus and reached a peak at day 7 in the oviducts; again, no bacteria were detectable on day 30. The inflammatory activity in the various organs of the FGT is likely important. Clinically relevant tissue damage occurs especially in the oviduct, where scarring compromises its function and leads to blockade of the passage and to hydrosalpinx, a dilation of the oviducts through fluid retention. Loss of oviduct function causes infertility. Severe inflammation in the adjacent uterine horns may have similar effects.

cNK cells were found at high abundance, especially in the uterine horns (Fig. 2A). However, relative to the size of the organs (expressed as cells per mg tissue), cNK cells were most abundantly found in the oviduct/ovary (oviduct) tissue (Fig. 2A). cNK cells were, however, found at only very low numbers on day 30, indicating a transient role. trNK cells were mostly located in the uterine horns, and their numbers showed little variation, although a small increase in the oviduct around 7 days postinfection (dpi) was seen (Fig. 2B). The continuous increase of ILC1 over 30 days was mostly confined to the uterine horns, with a transient accumulation in the oviduct that had almost resolved on day 30 (Fig. 2C). ILC2s, although at lower numbers, were also found, especially in the oviduct on day 7 (Fig. 2D). Overall, little ILC accumulation was seen in the cervix (Fig. 2). The results suggest that the inflammatory responses at the uterine horns versus the oviduct follow different kinetics and are not strictly determined by the actual bacterial presence.

NK cells are important producers of IFN-γ. ILC1 can produce both TNF and IFN-γ (32). We measured the production of TNF and IFN-γ by group 1 ILCs (NK cells and ILC1s) by flow cytometry. Few cells produced TNF at any of the tested time points; ILC1s were the main producers, with about 5% of cells expressing detectable TNF protein on day 4 (Fig. 3A to C). The proportion of cells producing IFN-γ reached about 15% to 20% in cNK cells, trNK cells, and ILC1s (Fig. 3D to F); the absolute numbers of the cells are given in Fig. 3G to I. The most surprising aspect here was that cytokine production had a clear peak earlier on, and hardly any cells produced IFN-γ on day 30, despite the continued presence (NK cells) or even continuous numerical expansion

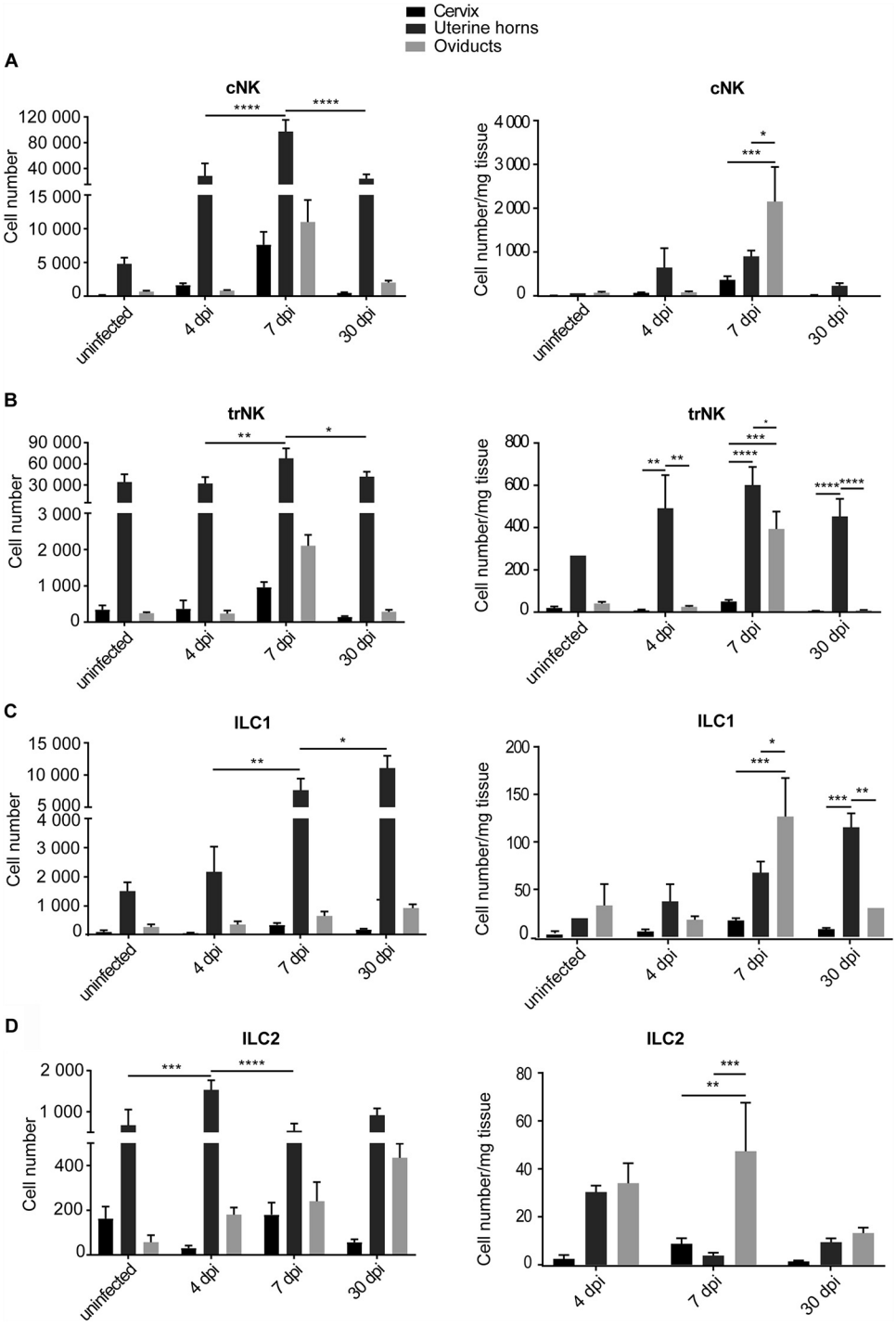

FIG 2 Dynamics of ILC numbers in FGT parts per mg tissue upon infection with *C. muridarum*. wt mice were infected intravaginally with 5×10^5 IFUs of *C. muridarum*. FGTs were isolated at the indicated time points, and leucocytes of the various FGT parts were analyzed by immunostaining and flow cytometry. Absolute cell numbers were obtained by including a defined number of reference beads and are represented relative to the corresponding tissue weight. (A) cNK cells were defined as $CD45^+$, Lin(CD3, CD5, CD19, TCRβ, TCR$\gamma\delta$, F4/80, FcεR1α, Ly6G)$^-$, $NK1.1^+$, $Eomes^+$, $CD49a^-$ cells. (B) trNK cells were defined as $CD45^+$, Lin^-, $NK1.1^+$, $Eomes^+$, $CD49a^+$ cells. (C) ILC1s were defined as $CD45^+$, Lin^-, $NK1.1^+$, $Eomes^-$, $CD49a^+$ cells. (D) ILC2s were defined as $CD45^+$, Lin^-, $CD127^+$, $ST2^+$, $GATA3^+$ cells. Panels on the left give total cell numbers and panels on the give cell numbers per tissue weight. Data show means and SEM of 3 to 9 mice (only two mice for uninfected uterine horns, group 1 ILCs). The numbers of mice and experiments are separately listed in Table S1. Significance between means was tested by Tukey's multiple-comparison test (*, $P < 0.05$; other differences were not significant). ILC, innate lymphoid cell; cNK, conventional natural killer; trNK, tissue-resident natural killer; dpi, days postinfection.

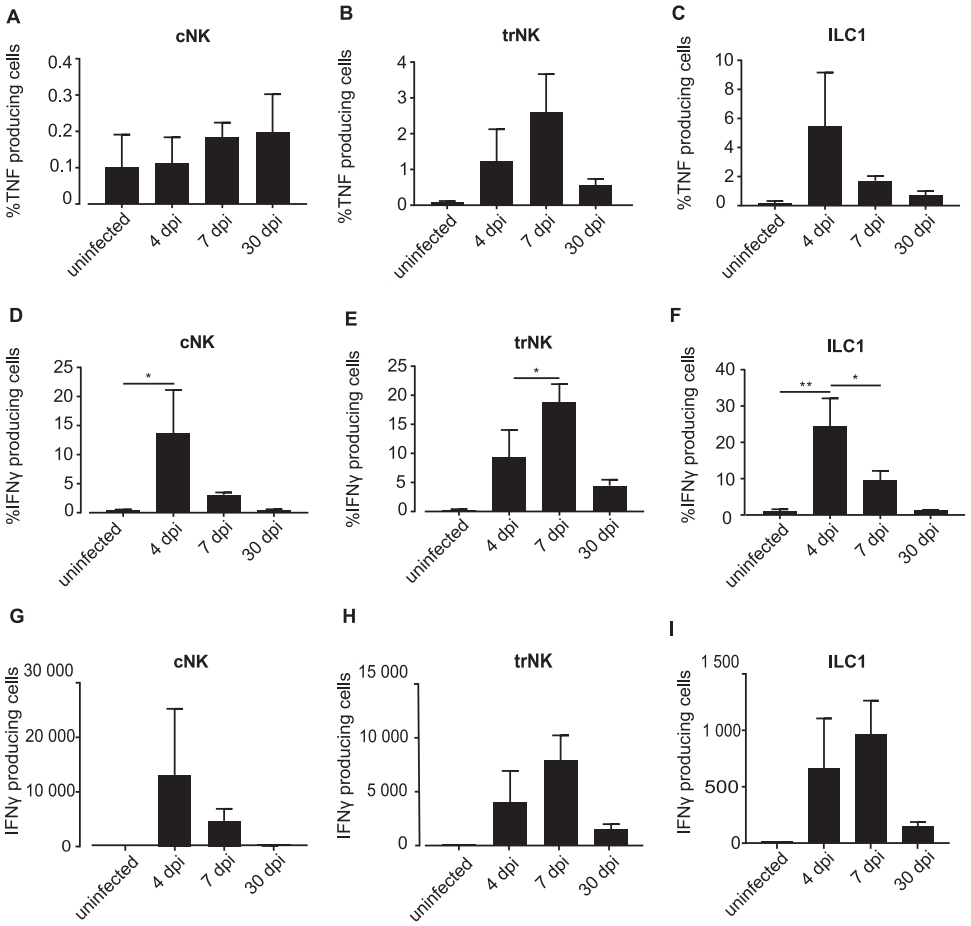

FIG 3 IFN-γ and TNF production by group1 ILCs upon infection with *C. muridarum*. wt mice were infected intravaginally with 5×10^5 IFUs of *C. muridarum*. FGTs were isolated at indicated time points and leucocytes of FGT uterine horns were analyzed via immunostaining and subsequent flow cytometry. TNF (A to C) and IFN-γ (D to I) production of group 1 ILCs. cNK cells were defined as CD45$^+$, Lin(CD3, CD5, CD19, TCRβ, TCR$\gamma\delta$, F4/80, FcεR1α, Ly6G)$^-$, NK1.1$^+$, Eomes$^+$, CD49a$^-$ cells. trNK cells were defined as CD45$^+$, Lin$^-$, NK1.1$^+$, Eomes$^+$, CD49a$^+$ cells. ILC1s were defined as CD45$^+$, Lin$^-$, NK1.1$^+$, Eomes$^-$, CD49a$^+$ cells. Percentages (D to F) and absolute numbers (G to I) of cells positive for gamma interferon (IFN-γ). Data show means and SEM of 6 to 9 mice. The exact numbers of mice and experiments are separately listed in Table S1. Significance between means was tested by Sidak's multiple-comparison test (*, $P < 0.05$; other differences were not significant). ILC, innate lymphoid cell; cNK, conventional natural killer; trNK, tissue-resident natural killer, dpi, days postinfection.

(ILC1s) of the cells. We attempted to study ILC1 function during *C. muridarum* infection by the use of *ncr1*-deficient mice, which had been reported to have a severe reduction in ILC1s (NCR1-$^{GFP/GFP}$ mice [33]). However, in our colony, these mice had, unexpectedly, normal numbers of cNK and ILC1s, with a minor reduction in trNK cells in their FGT (Fig. S5), and were therefore not suitable for this purpose.

We next measured the expression of cytokines known to activate ILCs by PCR in FGT tissue. An increase in IL-15, known to activate group 1 ILCs, was detectable on day 4 and, surprisingly, again on day 21, especially in the uterine horn. IL-18, also a group 1 ILC-activating cytokine, was also measured, but there were no significant changes, while IL-33, an ILC2-activating cytokine, was elevated on day 4 (Fig. 4).

To understand the role of ILCs as part of the reacting immune system, we infected mouse strains with deficiencies in immune cell populations with *C. muridarum* and monitored the dynamics of ILC populations. RAG1-deficient mice (which have no B or T cells) had normal group 1 ILC and ILC2s when uninfected, but group 1 ILCs expanded more strongly, while the ILC2 population in RAG1-deficient mice did not contract at the end of the first week as it did in wild-type (wt) mice (Fig. 5A to C; because RAG1-deficient mice cannot clear the infection, we did not analyze later time points).

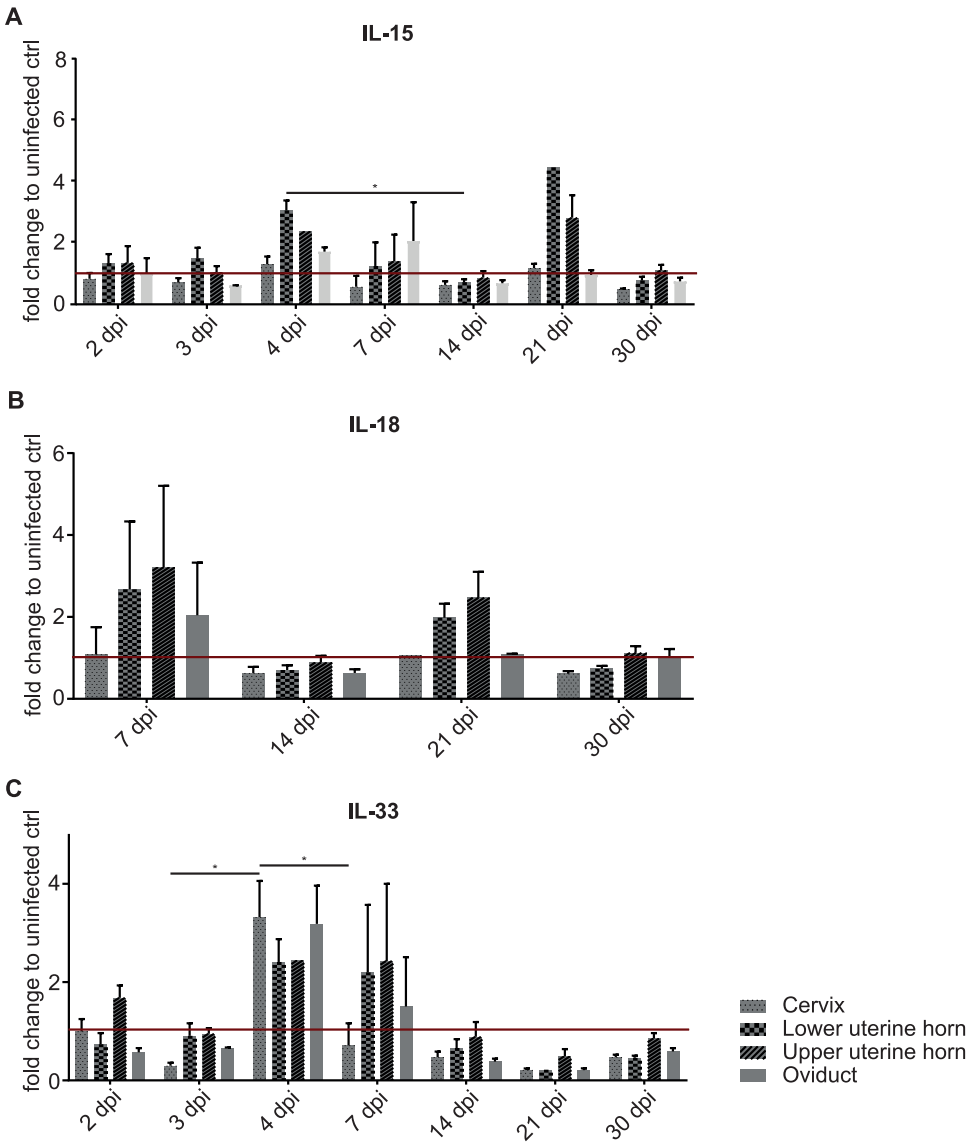

FIG 4 mRNA levels of ILC-activating cytokines in wt mice upon infection with *C. muridarum*. wt mice were infected intravaginally with 5×10^5 IFUs of *C. muridarum*. FGTs were isolated at the indicated time points, and RNA was obtained from the various FGT parts for quantitative PCR (qPCR). Relative mRNA levels of interleukin 15 (IL-15) (A), IL-18 (B), and IL-33 (C) (normalized to β-actin) are shown. Data show means and SEM of 3 to 9 mice (only two mice for cervix d21 IL-18). The exact numbers of mice and experiments are separately listed in Table S1. Significance between means was tested by Tukey's multiple-comparison test (*, $P < 0.05$; other differences were not significant). dpi, days postinfection; ctrl, control.

A salient feature of the early response to *C. muridarum* infection is the accumulation and activation of myeloid cells in the FGT (9). We therefore used a mouse model in which myeloid cells show a strongly reduced response to the infection. The chemokine receptor CCR2 is expressed by inflammatory monocytes, and mice deficient in CCR2 have lower numbers of monocytes in blood and in infected organs, presumably due to reduced egress of the cells from the bone marrow (34). Upon *C. muridarum* infection, there was a massive accumulation of monocytes in the FGT during the first week, but monocyte numbers were reduced to about 1% of those in the wt in CCR2-deficient mice (Fig. S6B). Neutrophils were less strongly reduced in these mice (about 5-fold) (Fig. S6C). We observed reductions in NK and ILC1 numbers in CCR2-deficient mice, but only early on (day 4) and only by about half (Fig. 5D and E); a reduction in ILC2s was

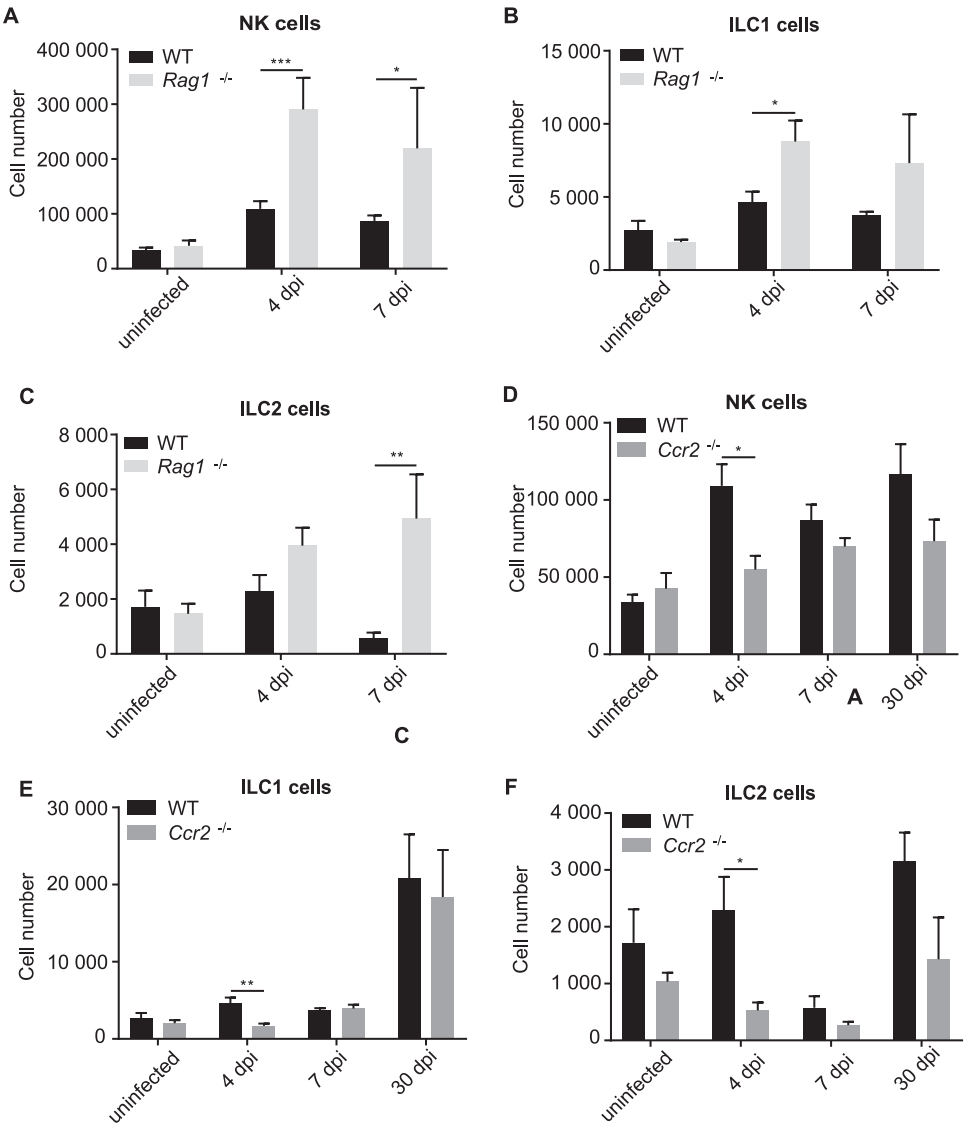

FIG 5 Dynamics of ILC numbers in whole FGTs comparing WT, RAG1$^{-/-}$, and Ccr2$^{-/-}$ mice upon infection with *C. muridarum*. wt, RAG1$^{-/-}$, and *Ccr2*$^{-/-}$ mice were infected intravaginally with 5 $\times$ 10^5 IFUs of *C. muridarum*. FGTs were isolated at the indicated time points, and leucocytes of whole FGTs were analyzed via immunostaining and subsequent flow cytometry. Absolute cell numbers were obtained by including a defined number of reference beads. (A to C) Comparison of wt and RAG1$^{-/-}$ mice. (D to F) Comparison of wt and CCR2$^{-/-}$ mice. (A, D) NK cells were defined as CD45$^+$, Lin(CD3, CD5, CD19, TCRβ, TCR$\gamma\delta$, F4/80, FcεR1α, Ly6G)$^-$, NK1.1$^+$, Eomes$^+$ cells. (B, E) ILC1s were defined as CD45$^+$, Lin$^-$, NK1.1$^+$, Eomes$^-$ cells. (C, F) ILC2s were defined as CD45$^+$, Lin$^-$, CD127$^+$, ST2$^+$, GATA3$^+$ cells. Data show means and SEM of 3 to 9 mice. The exact numbers of mice and experiments are separately listed in Table S1. Significance between means was tested by unpaired *t* test (*, $P = 0.05$). All statistically significant differences are indicated.

also seen (Fig. 5F). Myeloid cells, which are recruited rapidly upon *C. muridarum* infection, thus contribute to the accumulation of ILCs at the earlier stages of the infection.

We finally investigated the association of ILC presence with tissue damage upon *C. muridarum* infection. Tissue destruction in this model can be macroscopically observed from about 3 weeks on and exacerbates at later stages, although bacteria are undetectable during this time (Fig. S4). One relevant form of tissue damage is the inflammation-associated scarring of the oviduct that leads to hydrosalpinx. Of 49 mice analyzed on day 30, 30 had developed hydrosalpinx, 15 of them two-sided. Using oviduct tissue weight as a quantitative indicator of inflammation, we found clear and significant positive correlations between inflammation and the individual presences of NK, ILC1s and ILC2s (Fig. 6A to D). No significant correlation was found between CD45-negative

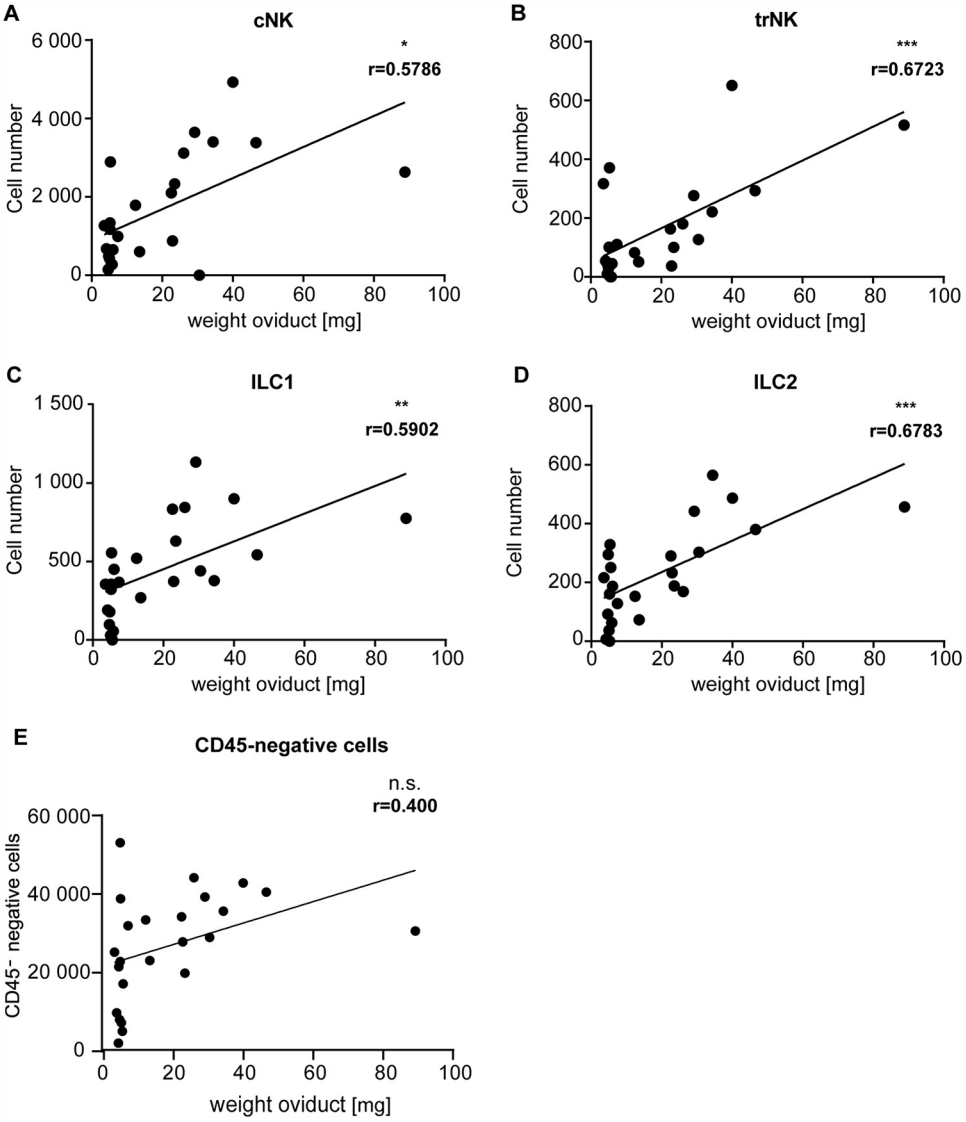

FIG 6 Correlation of the absolute numbers of ILCs or CD45-negative cells and the corresponding oviduct weight. wt mice were infected intravaginally with 5×10^5 IFUs of *C. muridarum*. FGTs were isolated at 30 dpi, and leucocytes of FGT oviducts were analyzed via immunostaining and subsequent flow cytometry. Data points represent the absolute number of cells in the oviduct, which were obtained by including a defined number of reference beads, and corresponding oviduct weights. (A) cNK cells were defined as $CD45^+$, Lin(CD3, CD5, CD19, TCRβ, TCR$\gamma\delta$, F4/80, FcεR1α, Ly6G)$^-$, $NK1.1^+$, $Eomes^+$, $CD49a^-$ cells. (B) trNK cells were defined as $CD45^+$, Lin^-, $NK1.1^+$, $Eomes^+$, $CD49a^+$ cells. (C) ILC1s were defined as $CD45^+$, Lin^-, $NK1.1^+$, $Eomes^-$, $CD49a^+$ cells. (D) ILC2s were defined as $CD45^+$, Lin^-, $CD127^+$, $ST2^+$, $GATA3^+$ cells. (E) Nonhematopoietic cells were defined as CD45 negative. The exact numbers of mice and experiments are separately listed in Table S1. Significance was tested by linear regression (*, $P < 0.05$; **, $P < 0.01$; ***, $P < 0.001$; n.s., $P > 0.05$). ILC, innate lymphoid cell; cNK, conventional natural killer; trNK, tissue-resident natural killer.

(nonimmune) cells and tissue weight (Fig. 6E). However, similar correlations were observed for neutrophils, monocytes, and T cells (Fig. S7), suggesting that general, sustained inflammatory activity involving various immune cells—rather than the activity of individual cell populations—contributes to chronic inflammation. A strong correlation between the weight of the uterine horns and the presence of cNK cells and ILC1s was observed, and, less strongly, with the presence of trNK cells and ILC2s (Fig. S8).

DISCUSSION

This study provides an analysis of the dynamics of ILC populations in the FGT within the immune response during the infection with *C. muridarum*. While NK cells were the

largest population of ILCs, ILC1s also accumulated substantially, and ILC3s made an interesting contribution through their conversion into ILC1s; ILC2s were present in relatively low numbers. The kinetics differed not only between ILC populations but also within the various organs of the FGT; cNK cells, ILC1s, and ILC2s all accumulated, especially in the oviducts. ILC population dynamics partly depended on other immune cell populations. The results suggest that ILCs are part of the complex immune and inflammatory response to chlamydial genital infection.

Other models have shown, using parabiotic mice, that ILC populations other than cNK cells expand locally rather than through recruitment from the blood; only in a chronic (worm) infection were ILC2s also recruited (35). Injection of human ILC precursor cells into alymphoid mice also supports this concept of tissue residency (36). Similarly, uterine trNK cells have been demonstrated to be a distinct, tissue-resident population (37); even during chlamydial infection in the model we used, this population expanded only mildly. Inhibition of apoptosis by the transgenic expression of Bcl-2 had no major impact, suggesting that mitochondrial apoptosis, which regulates population size in many types of immune reaction, does not substantially contribute to the dynamics of population size. The contribution of uterine NK cells to *C. muridaum* infection has been tested previously. YAC cell cytotoxicity (which measures NK cell activity) was observed in a previous study; the same study found that depleting NK cells (and some additional cell populations) with anti-asialo-GM antibody reduced IFN-γ secretion and led to an increase in bacterial load (21). NK1.1-positive cells have been found to secrete IFN-γ during the first week of infection (38). Depleting NK1.1-positive cells (group 1 ILC) prior to infection had no major effect on numbers of bacteria shed from the cervix of infected mice (39), although it enabled intestinal colonization of mice with an IFN-γ-sensitive strain of *C. muridarum* (23). Uterine trNK cells were described a few years ago as a separate lineage of NK cells (37). As expected, the variation in NK cell numbers during *C. muridarum* infection was largely in the cNK population, which expanded about 20-fold during the first week. Both NK cell populations produced IFN-γ—although at a rather low frequency of about 20%—but this did not correlate well with either the presence of bacteria or the recruitment of the cells. There was strong ongoing recruitment of cNK cells between days 4 and 7 postinfection, and an increase in bacterial number. However, by day 7, less than 5% of cNK cells (but 20% of trNK cells) produced IFN-γ. Even more strikingly, about 25% of ILC1s produced IFN-γ on day 4, but almost none did on day 30, although the accumulation of the cells continued until at least day 30. This suggests two conclusions, as follows: first, there may be a different localization, with different exposure to bacteria and other activating cells (epithelial cells, myeloid cells, and T cells) of the three types of group 1 ILC. Second, it appears that recruited cells are either inactive or have some other activity. Although by mRNA expression pattern, resting uterine trNK cells cluster more closely with ILC1s than with cNK cells (18), their reaction patterns in terms of accumulation and cytokine production were rather different. The ILC1 population that accumulates during *C. muridarum* infection may be functionally different from the small resident ILC1 population. Approaches permitting more comprehensive single-cell resolution of cell activity will be necessary to clarify their activity, and a better anatomical resolution of the immune response in the tissue will be necessary for understanding infection.

ILC2s were found at relatively low numbers only, and a significant increase in their number was only seen on day 4 in the uterine horns. Like cNK cells and ILC1s, ILC2s accumulated to relatively high densities in the oviduct tissue on day 7. ILC2s, activated by IL-33, have been shown to contribute to fibrosis in the lung (40) and liver (41), and IL-33 mRNA was increased in the cervix but not in other regions of the FGT on day 4. Fibrosis of the oviducts is a key mechanism of tissue damage in *C. muridarum* infection (42). It is therefore conceivable that ILC2s contribute to tissue damage during chlamydial infection. The continued presence, and sometimes numerical increase, of most ILC types at the late stages of chlamydial infection is indeed remarkable. All other cell types—myeloid cells and T cells—that are present in this infection are already strongly

reduced at those time points (10). This may mean that ILCs indeed contribute to tissue remodeling and destruction, which is mostly seen from day 30 onwards.

In the intestine, ILC3s support inflammation (28) and provide protection against a bacterial infection (27). In the FGT, there were very few (under 500 per mouse) ILC3s, and although cells were recruited, about 80% to 90% were converted to ILC1s during the course of the infection. This transdifferentiation has been observed previously in inflammatory conditions, for instance, under the influence of IL-12 (29), and it may well have a functional consequence because exRORγt-ILC3s have lost the ability to produce ILC3 cytokines.

Accumulation of NK cells and ILC2s, but less so that of ILC1s, was reduced in CCR2-deficient mice upon *C. muridarum* infection, most likely as an effect secondary to the lack of myeloid cells. This suggests that the myeloid-cell-caused inflammation is a factor in the recruitment and expansion of ILCs. The known ILC-activating cytokines were observed at low levels, but at this stage we do not know which cell type produces them. It does seem clear, however, that ILCs react as part of a complex inflammatory and immune reaction to the infection, which likely involves a contribution from infected epithelial cells, reacting myeloid cells, and also T cells. We have not been able specifically to deplete ILC populations thus far. In our opinion, the data do suggest that ILCs make a contribution, especially at later stages of the resolution of the inflammation, when tissue repair and restructuring occur.

MATERIALS AND METHODS

Bacteria. *Chlamydia muridarum* (strain 03DC39; kindly provided by Konrad Sachse, Jena) was propagated in HeLa cells upon spin infection (2,600 × *g* for 1 h). Bacteria were purified upon mechanical cell lysis by centrifugation (20,000 × *g* for 3.5 h at 4°C). Purified chlamydiae were stored at −80°C.

Mouse strains. C57BL/6NRj mice were purchased from Janvier Laboratories. *vav-bcl-2* transgenic mice (25) were a gift from Jerry Adams, Melbourne. Mice deficient for *Ccr2* (43) were kindly provided by Philipp Henneke (Freiburg, Germany). To obtain Eomes and RORγt-fm reporter mice, *Eomes*$^{GFP/+}$ *Rosa26*$^{YFP/+}$ and *Rorc(γt)*-Cre^{tg} (44–46) mice were crossbred. Mice deficient for *Rag1* were obtained from an internal breeding of the Uniklinik Freiburg. *Ncr1*$^{GFP/GFP}$ (*Ncr1*^{tm1Oman}/J) mice (33) were purchased from Jackson Laboratories.

Chlamydial infection. Female mice were injected intravaginally with 2.5 mg of medroxyprogesterone (Depo-Clinovir; Pfizer) at 10 and 3 days before infection with 5×10^5 inclusion-forming units (IFUs) of *C. muridarum*. Uninfected control mice were treated with medroxyprogesterone, and phosphate-buffered saline (PBS) was inoculated intravaginally. All animal experiments were approved by the Regierungspräsidium Freiburg.

Flow cytometry. FGTs were mechanically disrupted and enzyme digested. Leucocytes were isolated, and immunostaining was performed (for details, see "Supplemental Methods" in the supplemental material).

Quantitative PCR. FGT parts were homogenized, and RNA was isolated. RNA was transcribed into cDNA to subsequently perform quantitative PCR (qPCR). Fold change expression levels were determined relative to uninfected mice by calculating comparative threshold cycle ($\Delta\Delta C_T$) values after normalization to the reference gene *β-actin* (details in "Supplemental Methods" in the supplemental material).

Detection of *C. muridarum* genome copies in FGT tissue. Tissue digestion and DNA isolation were performed to subsequently perform qPCR. C_T values were used to determine chlamydial genome copies utilizing the equation of the standard curve. The standard curve was generated via DNA isolation of a defined number of IFUs of *C. muridarum* and subsequent qPCR (details in "Supplemental Methods" in the supplemental material).

Statistical analysis. Data show means and standard error of the mean (SEM), and statistical analyses were performed using Tukey's multiple-comparison test, Sidak's multiple-comparison test, unpaired *t* test, or Pearson's correlation coefficient. Statistical evaluation was performed with Prism (GraphPad Software, Inc., USA). A *P* value of <0.05 was considered statistically significant.

SUPPLEMENTAL MATERIAL

Supplemental material is available online only.

SUPPLEMENTAL FILE 1, PDF file, 0.7 MB.

SUPPLEMENTAL FILE 2, PDF file, 0.3 MB.

SUPPLEMENTAL FILE 3, PDF file, 0.5 MB.

ACKNOWLEDGMENTS

We thank Philipp Henneke for providing the strain of CCR2-deficient mice.

We declare no competing interests.

This work was supported by the Deutsche Forschungsgemeinschaft (grant DFG 2128/20-1 to G.H.).

REFERENCES

1. Newman L, Rowley J, Vander Hoorn S, Wijesooriya NS, Unemo M, Low N, Stevens G, Gottlieb S, Kiarie J, Temmerman M. 2015. Global estimates of the prevalence and incidence of four curable sexually transmitted infections in 2012 based on systematic review and global reporting. PLoS One 10:e0143304. https://doi.org/10.1371/journal.pone.0143304.
2. Huai P, Li F, Chu T, Liu D, Liu J, Zhang F. 2020. Prevalence of genital *Chlamydia trachomatis* infection in the general population: a meta-analysis. BMC Infect Dis 20:589. https://doi.org/10.1186/s12879-020-05307-w.
3. Bakken IJ, Skjeldestad FE, Lydersen S, Nordbo SA. 2007. Births and ectopic pregnancies in a large cohort of women tested for *Chlamydia trachomatis*. Sex Transm Dis 34:739–743. https://doi.org/10.1097/01.olq.0000261326.65503.f6.
4. Darville T, Hiltke TJ. 2010. Pathogenesis of genital tract disease due to *Chlamydia trachomatis*. J Infect Dis 201:S114–S125. https://doi.org/10.1086/652397.
5. Geisler WM, Lensing SY, Press CG, Hook EW. 3rd, 2013. Spontaneous resolution of genital *Chlamydia trachomatis* infection in women and protection from reinfection. J Infect Dis 207:1850–1856. https://doi.org/10.1093/infdis/jit094.
6. Stary G, Olive A, Radovic-Moreno AF, Gondek D, Alvarez D, Basto PA, Perro M, Vrbanac VD, Tager AM, Shi J, Yethon JA, Farokhzad OC, Langer R, Starnbach MN, von Andrian UH. 2015. A mucosal vaccine against *Chlamydia trachomatis* generates two waves of protective memory T cells. Science 348:aaa8205. https://doi.org/10.1126/science.aaa8205.
7. Gupta K, Bakshi RK, Van Der Pol B, Daniel G, Brown L, Press CG, Gorwitz R, Papp J, Lee JY, Geisler WM. 2018. Repeated *Chlamydia trachomatis* infections are associated with lower bacterial loads. Epidemiol Infect 147:e18. https://doi.org/10.1017/S0950268818002704.
8. Farris CM, Morrison RP. 2011. Vaccination against *Chlamydia* genital infection utilizing the murine *C. muridarum* model. Infect Immun 79:986–996. https://doi.org/10.1128/IAI.00881-10.
9. Murthy AK, Li W, Ramsey KH. 2018. Immunopathogenesis of chlamydial infections. Curr Top Microbiol Immunol 412:183–215. https://doi.org/10.1007/82_2016_18.
10. Zortel T, Schmitt-Graeff A, Kirschnek S, Hacker G. 2018. Apoptosis modulation in the immune system reveals a role of neutrophils in tissue damage in a murine model of chlamydial genital infection. J Infect Dis 217:1832–1843. https://doi.org/10.1093/infdis/jiy126.
11. Yu H, Lin H, Xie L, Tang L, Chen J, Zhou Z, Ni J, Zhong G. 2019. *Chlamydia muridarum* induces pathology in the female upper genital tract via distinct mechanisms. Infect Immun 87:e00145-19. https://doi.org/10.1128/IAI.00145-19.
12. Murthy AK, Li W, Chaganty BK, Kamalakaran S, Guentzel MN, Seshu J, Forsthuber TG, Zhong G, Arulanandam BP. 2011. Tumor necrosis factor alpha production from $CD8^+$ T cells mediates oviduct pathological sequelae following primary genital *Chlamydia muridarum* infection. Infect Immun 79:2928–2935. https://doi.org/10.1128/IAI.05022-11.
13. Manam S, Thomas JD, Li W, Maladore A, Schripsema JH, Ramsey KH, Murthy AK. 2015. Tumor necrosis factor (TNF) receptor superfamily member 1b on $CD8^+$ T cells and TNF receptor superfamily member 1a on non-$CD8^+$ T cells contribute significantly to upper genital tract pathology following chlamydial infection. J Infect Dis 211:2014–2022. https://doi.org/10.1093/infdis/jiu839.
14. Vivier E, Artis D, Colonna M, Diefenbach A, Di Santo JP, Eberl G, Koyasu S, Locksley RM, McKenzie ANJ, Mebius RE, Powrie F, Spits H. 2018. Innate lymphoid cells: 10 years on. Cell 174:1054–1066. https://doi.org/10.1016/j.cell.2018.07.017.
15. Kotas ME, Locksley RM. 2018. Why innate lymphoid cells? Immunity 48:1081–1090. https://doi.org/10.1016/j.immuni.2018.06.002.
16. Cording S, Medvedovic J, Lecuyer E, Aychek T, Eberl G. 2018. Control of pathogens and microbiota by innate lymphoid cells. Microbes Infect 20:317–322. https://doi.org/10.1016/j.micinf.2018.05.003.
17. Doisne JM, Balmas E, Boulenouar S, Gaynor LM, Kieckbusch J, Gardner L, Hawkes DA, Barbara CF, Sharkey AM, Brady HJ, Brosens JJ, Moffett A, Colucci F. 2015. Composition, development, and function of uterine innate lymphoid cells. J Immunol 195:3937–3945. https://doi.org/10.4049/jimmunol.1500689.
18. Filipovic I, Chiossone L, Vacca P, Hamilton RS, Ingegnere T, Doisne JM, Hawkes DA, Mingari MC, Sharkey AM, Moretta L, Colucci F. 2018. Molecular definition of group 1 innate lymphoid cells in the mouse uterus. Nat Commun 9:4492. https://doi.org/10.1038/s41467-018-06918-3.
19. Ashkar AA, Rosenthal KL. 2003. Interleukin-15 and natural killer and NKT cells play a critical role in innate protection against genital herpes simplex virus type 2 infection. J Virol 77:10168–10171. https://doi.org/10.1128/jvi.77.18.10168-10171.2003.
20. Crespo AC, Mulik S, Dotiwala F, Ansara JA, Sen Santara S, Ingersoll K, Ovies C, Junqueira C, Tilburgs T, Strominger JL, Lieberman J. 2020. Decidual NK cells transfer granulysin to selectively kill bacteria in trophoblasts. Cell 182:1125–1139.e1118. https://doi.org/10.1016/j.cell.2020.07.019.
21. Tseng CT, Rank RG. 1998. Role of NK cells in early host response to chlamydial genital infection. Infect Immun 66:5867–5875. https://doi.org/10.1128/IAI.66.12.5867-5875.1998.
22. Xu H, Su X, Zhao Y, Tang L, Chen J, Zhong G. 2020. Innate lymphoid cells are required for endometrial resistance to *Chlamydia trachomatis* infection. Infect Immun 88:e00152-20. https://doi.org/10.1128/IAI.00152-20.
23. He Y, Xu H, Song C, Koprivsek JJ, Arulanandam B, Yang H, Tao L, Zhong G. 2021. Adoptive transfer of group 3-like innate lymphoid cells restores mouse colon resistance to colonization of a gamma interferon-susceptible *Chlamydia muridarum* mutant. Infect Immun 89:e00533-20. https://doi.org/10.1128/IAI.00533-20.
24. Cotter TW, Ramsey KH, Miranpuri GS, Poulsen CE, Byrne GI. 1997. Dissemination of Chlamydia trachomatis chronic genital tract infection in gamma interferon gene knockout mice. Infect Immun 65:2145–2152. https://doi.org/10.1128/iai.65.6.2145-2152.1997.
25. Ogilvy S, Metcalf D, Print CG, Bath ML, Harris AW, Adams JM. 1999. Constitutive Bcl-2 expression throughout the hematopoietic compartment affects multiple lineages and enhances progenitor cell survival. Proc Natl Acad Sci U S A 96:14943–14948. https://doi.org/10.1073/pnas.96.26.14943.
26. Pellegrini M, Bouillet P, Robati M, Belz GT, Davey GM, Strasser A. 2004. Loss of Bim increases T cell production and function in interleukin 7 receptor-deficient mice. J Exp Med 200:1189–1195. https://doi.org/10.1084/jem.20041328.
27. Guo X, Qiu J, Tu T, Yang X, Deng L, Anders RA, Zhou L, Fu YX. 2014. Induction of innate lymphoid cell-derived interleukin-22 by the transcription factor STAT3 mediates protection against intestinal infection. Immunity 40:25–39. https://doi.org/10.1016/j.immuni.2013.10.021.
28. Buonocore S, Ahern PP, Uhlig HH, Ivanov II, Littman DR, Maloy KJ, Powrie F. 2010. Innate lymphoid cells drive interleukin-23-dependent innate intestinal pathology. Nature 464:1371–1375. https://doi.org/10.1038/nature08949.
29. Bal SM, Golebski K, Spits H. 2020. Plasticity of innate lymphoid cell subsets. Nat Rev Immunol 20:552–565. https://doi.org/10.1038/s41577-020-0282-9.
30. Klose CS, Kiss EA, Schwierzeck V, Ebert K, Hoyler T, d'Hargues Y, Goppert N, Croxford AL, Waisman A, Tanriver Y, Diefenbach A. 2013. A T-bet gradient controls the fate and function of CCR6-RORγ^+ innate lymphoid cells. Nature 494:261–265. https://doi.org/10.1038/nature11813.
31. Vonarbourg C, Mortha A, Bui VL, Hernandez PP, Kiss EA, Hoyler T, Flach M, Bengsch B, Thimme R, Holscher C, Honig M, Pannicke U, Schwarz K, Ware CF, Finke D, Diefenbach A. 2010. Regulated expression of nuclear receptor RORγt confers distinct functional fates to NK cell receptor-expressing RORγt$^+$ innate lymphocytes. Immunity 33:736–751. https://doi.org/10.1016/j.immuni.2010.10.017.
32. Spits H, Artis D, Colonna M, Diefenbach A, Di Santo JP, Eberl G, Koyasu S, Locksley RM, McKenzie AN, Mebius RE, Powrie F, Vivier E. 2013. Innate lymphoid cells—a proposal for uniform nomenclature. Nat Rev Immunol 13:145–149. https://doi.org/10.1038/nri3365.
33. Wang Y, Dong W, Zhang Y, Caligiuri MA, Yu J. 2018. Dependence of innate lymphoid cell 1 development on NKp46. PLoS Biol 16:e2004867. https://doi.org/10.1371/journal.pbio.2004867.
34. Tsou CL, Peters W, Si Y, Slaymaker S, Aslanian AM, Weisberg SP, Mack M, Charo IF. 2007. Critical roles for CCR2 and MCP-3 in monocyte mobilization from bone marrow and recruitment to inflammatory sites. J Clin Invest 117:902–909. https://doi.org/10.1172/JCI29919.

35. Gasteiger G, Fan X, Dikiy S, Lee SY, Rudensky AY. 2015. Tissue residency of innate lymphoid cells in lymphoid and nonlymphoid organs. Science 350:981–985. https://doi.org/10.1126/science.aac9593.
36. Lim AI, Li Y, Lopez-Lastra S, Stadhouders R, Paul F, Casrouge A, Serafini N, Puel A, Bustamante J, Surace L, Masse-Ranson G, David E, Strick-Marchand H, Le Bourhis L, Cocchi R, Topazio D, Graziano P, Muscarella LA, Rogge L, Norel X, Sallenave JM, Allez M, Graf T, Hendriks RW, Casanova JL, Amit I, Yssel H, Di Santo JP. 2017. Systemic human ILC precursors provide a substrate for tissue ILC differentiation. Cell 168:1086–1100.e1010. https://doi.org/10.1016/j.cell.2017.02.021.
37. Sojka DK, Plougastel-Douglas B, Yang L, Pak-Wittel MA, Artyomov MN, Ivanova Y, Zhong C, Chase JM, Rothman PB, Yu J, Riley JK, Zhu J, Tian Z, Yokoyama WM. 2014. Tissue-resident natural killer (NK) cells are cell lineages distinct from thymic and conventional splenic NK cells. Elife 3:e01659. https://doi.org/10.7554/eLife.01659.
38. Nagarajan UM, Sikes J, Prantner D, Andrews CW, Jr, Frazer L, Goodwin A, Snowden JN, Darville T. 2011. MyD88 deficiency leads to decreased NK cell gamma interferon production and T cell recruitment during *Chlamydia muridarum* genital tract infection, but a predominant Th1 response and enhanced monocytic inflammation are associated with infection resolution. Infect Immun 79:486–498. https://doi.org/10.1128/IAI.00843-10.
39. Naglak EK, Morrison SG, Morrison RP. 2017. Neutrophils are central to antibody-mediated protection against genital chlamydia. Infect Immun 85:e00409-17. https://doi.org/10.1128/IAI.00409-17.
40. Li D, Guabiraba R, Besnard AG, Komai-Koma M, Jabir MS, Zhang L, Graham GJ, Kurowska-Stolarska M, Liew FY, McSharry C, Xu D. 2014. IL-33 promotes ST2-dependent lung fibrosis by the induction of alternatively activated macrophages and innate lymphoid cells in mice. J Allergy Clin Immunol 134:1422–1432.e1411. https://doi.org/10.1016/j.jaci.2014.05.011.
41. McHedlidze T, Waldner M, Zopf S, Walker J, Rankin AL, Schuchmann M, Voehringer D, McKenzie AN, Neurath MF, Pflanz S, Wirtz S. 2013. Interleukin-33-dependent innate lymphoid cells mediate hepatic fibrosis. Immunity 39:357–371. https://doi.org/10.1016/j.immuni.2013.07.018.
42. Shah AA, Schripsema JH, Imtiaz MT, Sigar IM, Kasimos J, Matos PG, Inouye S, Ramsey KH. 2005. Histopathologic changes related to fibrotic oviduct occlusion after genital tract infection of mice with *Chlamydia muridarum*. Sex Transm Dis 32:49–56. https://doi.org/10.1097/01.olq.0000148299.14513.11.
43. Kurihara T, Warr G, Loy J, Bravo R. 1997. Defects in macrophage recruitment and host defense in mice lacking the CCR2 chemokine receptor. J Exp Med 186:1757–1762. https://doi.org/10.1084/jem.186.10.1757.
44. Srinivas S, Watanabe T, Lin CS, William CM, Tanabe Y, Jessell TM, Costantini F. 2001. Cre reporter strains produced by targeted insertion of *EYFP* and *ECFP* into the ROSA26 locus. BMC Dev Biol 1:4. https://doi.org/10.1186/1471-213x-1-4.
45. Eberl G, Littman DR. 2004. Thymic origin of intestinal $\alpha\beta$ T cells revealed by fate mapping of RORγt^{+} cells. Science 305:248–251. https://doi.org/10.1126/science.1096472.
46. Arnold SJ, Sugnaseelan J, Groszer M, Srinivas S, Robertson EJ. 2009. Generation and analysis of a mouse line harboring GFP in the Eomes/Tbr2 locus. Genesis 47:775–781. https://doi.org/10.1002/dvg.20562.